Czech Technical University in Prague
Faculty of Nuclear Sciences and Physical Engineering

Department of Physics

Modelling of magnetic equilibrium in tokamaks

RESEARCH TASK

Author: Martin Matušů
Supervisor: Ing. Jakub Urban, Ph.D.
Year: 2015

Insert ASSIGNMENT here.

Acknowledgement

I would like to thank my supervisor Ing. Jakub Urban, Ph.D. for his professional comments and for his help as well as patience by the time of my understanding of the CRONOS suite of codes. I would like to thank my close friends and family for the support they granted me as well.

Martin Matušů

Title:
Modelling of magnetic equilibrium in tokamaks

Author: Martin Matušů

Branch of study: Physics and Technology of Thermonuclear Fusion
Supervisor: Ing. Jakub Urban, Ph.D.
Institute of Plasma Physics of the Czech Academy of Sciences

Abstract: Thermonuclear fusion is a potential energy source for next few centuries. In order to control this process on Earth, it is necessary to simulate conditions of Sun core. All matter is in plasma state in these conditions and therefore a thermonuclear reactor is needed to create a environment for the plasma. Requirements on such a reactor are stated in Lawson criterion. Tokamak device is except other types of thermonuclear reactor close to meet the Lawson criterion. On the other hand, closer analysis of the Lawson criterion results in the need of scaling the tokamak device. Yet, large experiments like ITER and DEMO are expensive and need to be supported by numerical simulations of their function. Part of such simulations is the magnetic equilibrium solver, e.g. FREEBIE as a free-boundary equilibrium evolution solver module for the CRONOS suite of codes for complex discharge simulation. FREEBIE as a recent code is still in development used circuit equations description unable to solve complex circuits of power supply of poloidal components. This work substitutes this description by potential description of nodes, adding additional equations to the system. FREEBIE also needed module of fast equipotential finder in order to find closed flux surfaces, average plasma quantities over them and allow easy the coordinates transformation. This module is meant to use general spline so the consistence of FREEBIE code may be conserved.

Key words: Thermonuclear fusion, Plasma physics, Tokamak, Numerical modelling, MHD equilibrium

Contents

Introduction

World energy needs and nuclear power

Considering the speed of the growth of energy needs, humanity has to figure out how to solve this issue in the long term horizon. For a long time, burning fossil fuels has been a sufficient method to cover energy demands. But this method has two main problems, the scarcity of fuel and ecological consequences. The Manhattan project provided an alternative which was not essentially burdened by previous problems. But with the occurrence of accidents in fission power plants and a still growing energy demand, another source of energy is needed. With advanced knowledge of physics it may appear that renewable energy is the best way to solve this crisis. Although renewable energy may be the final solution of energetics problem of humanity, the technology to achieve this utopia is not sufficiently developed. Therefore there is a need to find a solution in this current period. A convenient source of energy has been found by understanding the Sun. In its centre, an enormous amount of energy is generated due to the process of fusion.

Chapter 1

The way to the fusion power plant

1.1 The fusion principle

The nuclear fusion is a process of combining two or more light atomic nuclei into a more complicated one. This results in an energy yield E according to the Einstein's equation

$$E = \Delta m c^2, \tag{1.1}$$

in which Δm stands for the mass difference of the reactants and the products of fusion and c is the constant of speed of light.

By combining two atomic nuclei is meant a fact of bringing them so close to each other that the strong interaction overcomes the coulomb repulsion of two positive nuclei. If the barrier of Coulomb interaction would be unaltered, the conditions of fusion would be quite hard to achieve and even stars would not produce energy. The explanation to the model of the Sun brought George Gamow in the early twentieth century as he explained alpha decay by quantum tunneling.

By applying his discovery to the problem of fusion the energy necessary to fuse two nuclei decreases dramatically. Thanks to its reaction rate values, the reaction of deuterium(D) and tritium(T) is the easiest to achieve. The ideal energy of the nuclei for the D-T reaction is 31 keV. Nuclei of this energy have the highest probability of tunneling through the barrier and thus fusing.

In order to achieve fusion in a commercial scale as the fusion power plant, the reasonable way to grant nuclei such energies is by increasing their chaotic energy by heating them. The ideal temperature of matter for the D-T fusion is approximately 30 keV, where 1 eV is an equivalent of 11600 K. At such high temperatures all matter considered as possible fusion fuel is in plasma state.

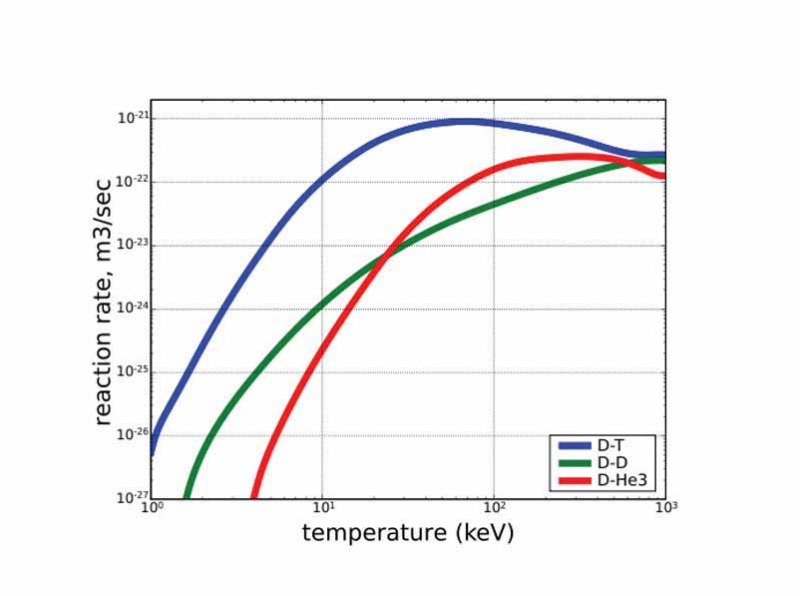

Figure 1.1: The dependency of the reaction rate at the fuel temperature; reprinted from [3].

1.2 Plasma

By heating the fusion fuel its chaotic energy rises. At certain point, electrons has energy to overcome the bound in the nuclei and starts to act separately. Therefore the plasma is a really complex system as it is no longer neutral and movement of one particle affects the whole plasma. On the other hand, every point charge in such system gets surrounded by particles of the opposite charge and thus its effect on longer range diminishes. Due to this principle, the plasma always neutralize any charge density irregularities. This characteristic of plasma is called quasi-neutrality.

Such a chaotic system is very unpredictable and therefore the thermonuclear reactor used to contain plasma matter in relative steady state is needed.

1.3 The Lawson criterion and its fulfillment

No matter what kind of reactor is build, it is necessary to consider its possible usage as a power plant. This idea was formulated in 1957 by J.D.Lawson as the Lawson criterion. It considers the power losses and gains in the reactor due to the additional heating of plasma, energy radiance by plasma and the fusion reaction itself. Additionally it describes

the moment of so called ignition, when the plasma loses P_L are compensated by internal sources(fusion gain) P_i. Its final form is an inequality unique for each fusion reaction, specially for D-T reaction

$$\tau_E \ \geq \ \frac{W_p}{P_L} \ = \ \frac{15(n_a + n_b)k_B T}{n_a n_b < \sigma v_r > \varepsilon_f}, \tag{1.2}$$

where n_a and n_b stand for densities of reaction reactants, k_B is a Boltzmann constant, σ stands for cross section, v_r is a relative velocity and ε_f is the energy gain of one reaction. Moreover, Lawson defined a variable called the confinement time τ_E describing the effectiveness of confinement of plasma energy

$$\tau_E \ = \ \frac{W_P}{P_L} \ = \ \frac{5W_P}{P_i}, \tag{1.3}$$

where W_P represents plasma energy and P_L its loses, which can be rewritten as a fifth of plasma internal gain (fusion) for the D-T fusion. Under these conditions and densities of fuel ($n_D \ = \ n_T \ = \ n/2$), the Lawson criterion may be rewritten as

$$\tau_E \ \geq \ \frac{60 k_B T}{n < \sigma v_r > \varepsilon_f}. \tag{1.4}$$

Especially for D-T fusion, it is often rewritten in the form of so called triple product

$$n \tau_E T \ \geq \ const, \tag{1.5}$$

which is only valid in the part around the minimum of the left hand side expression with respect to the temperature, yet the minimum is what is needed. The minimum of such function shows, at which temperature are the best conditions of reaching the fusion ignition.

1.4 The fusion reactor

Several methods of plasma containment were developed. The main of them are stellarators, tokamaks, pinches and inertial confinement. Generally they could be divided as magnetic confined plasma methods and inertial confinement. Considering the plasma power plant with continuous and stable energy output, the inertial confinement cannot be used as its drivers (the most spread drivers are lasers) energy input would be too high compared to the fusion output. Although both, stellarators and pinches, made significant scientific discoveries, they cannot match tokamaks at the field of the confinement time. Considering the Lawson criterion tokamaks are closest to fulfill it and thus become the method of future fusion power plant.

The tokamaks are axisymmetric toroidal devices which confines plasma with aid of a toroidal (in the toroid axis direction) electrical plasma current I_p and gains stability from

a strong guiding toroidal magnetic field B_t. Plasma current I_p with external poloidal (in toroidal geometry, creating poloidal magnetic field) coils generates poloidal (perpendicular to the toroid axis direction) magnetic field B_p.

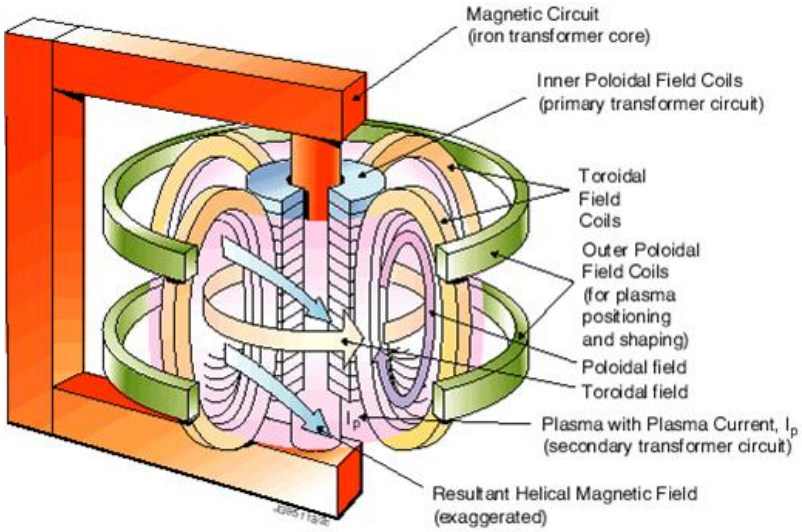

Figure 1.2: The basic principle of the tokamak magnetic field; reprinted from [13].

In order to reach the fusion in tokamaks, Lawson criterion respectively the triple product condition has to be fulfilled. As the ideal temperature is set by the peak of reaction rates of the considered reaction (fig.1.1) and the density is limited by the pressure limit. The only remaining way of fulfilling the triple product condition is therefore the energy confinement time τ_E. The energy confinement time quantity is hard to be calculated in theory. On the other hand fitting of the experimental data (1.3) yields quite clear formula

$$\tau_E \propto R^3 B_t P_H^{0.65}, \tag{1.6}$$

where P_H stands for the heating power. As the heating power and toroidal magnetic field as well have technical limits, the only way of fulfilling the triple product condition is by increasing the tokamak radius. Even by inventing any improvements which varies these dependencies, the main characteristic is always clear: the tripple product funcion rises with radius of the tokamak. Due to this fact, scaling of tokamaks is necessary and leads to the projects like JET, ITER and DEMO. By scaling the projects their maintance costs rises and therefore the simulations of discharges are necessary in order to partially predict the results and lower the reactor maintenance cost.

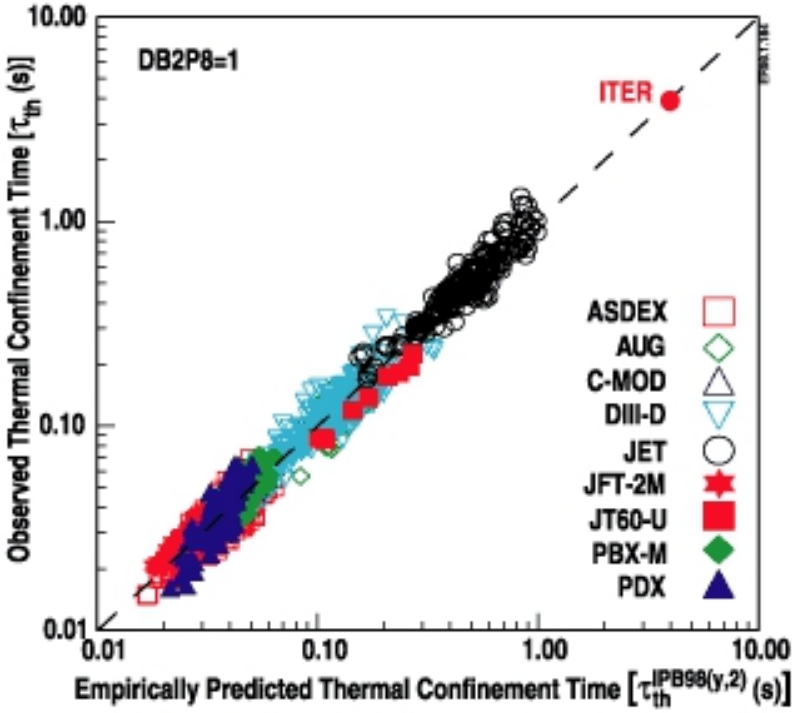

Figure 1.3: Fitting of the energy confinement time experimental results; reprinted from [2].

Chapter 2

Plasma simulation

As a very complex system, plasma is very difficult to be simulated. Moreover, the simulations differ by observed phenomena by scale of all dimensions. Considering the computational power of humanity nowadays, the simulation that would cover the whole state space (time, position and velocity) cannot describe large number of particles as standalone objects. Therefore, a lot of codes is necessary to study plasma on all dimensions and their comparison must obey the law scaling. When a complex simulation code is created, it has to be benchmarked to a verified code on the overlapping domain, e.g. code describing movement of single particles should yield the same results as a code describing group movement of plasma, if the amount of particles that both codes can handle is considered. Benchmarking of codes is therefore crucial for plasma simulation.

One of the special cases, which needs to be simulated are conditions in expensive facilities as mentioned in previous chapter. Even these simulations varies from description of the whole power plant system, including electrical grid system and power generation/consumption, to a discharge specific dimension describing time evolution of the reactor discharge. The first type must be run by discharge operator to set the limits granted by electrical grid and the latter type is needed in order to decide ideal physics specifics of the shot. However it is needed in future power-plant, the description of the electrical grid would require a dedicated review work and is outside the scope of this thesis. On the other hand, the simulation of physics inside the tokamak during a discharge is mandatory for plasma studies and interpreting the discharge results as well. Thanks to the comparison of differences between experiment results and simulation results, better understanding of observed phenomena is possible.

2.1 CRONOS

A lot of codes had been created so far in order to describe specific parts of tokamak discharge. Even though they all have results separately, they need to be benchmarked and

bound together in one platform, that handles physics workflow and data management of specific codes and normalize them in the way of compatibility. This needs were the motivation basis for the development of CRONOS suite of codes [1]. CRONOS itself is a part of European Fusion Development Agreement (EFDA), Integrated Tokamak Modelling Task Force (ITM-TF). Its main mission is to build a validated suite of simulation codes for ITER plasmas and provide a software infrastructure framework for EU integrated modelling activities.

The core of the CRONOS itself is a numerical solver of transport equations for various plasma fluid quantities. This core grants the time development of system and is connects in modular structure all other specific solvers such as 2D-equilibrium solver, radiation, particle and momentum sources/losses, etc. As the simulation has to yield same results as experiment, various feedback algorithms used in an experiment is integrated in CRONOS as well.

In order to preserve the consistence of modules, the CRONOS platform sets few restrictions both in physics, e.g. approximations and coordinates used in modules, and the numerical aspect of codes, e.g. precision of handled data.

Including many modules in modular structure grants CRONOS the possibility of replacing one of them by experiment measurement data. In this way, CRONOS does not work only as an predictive code, but as an interpretive code too. Comparing the real measurement data and using them as input for other validated modules results in diagnostics testing and possible calibration.

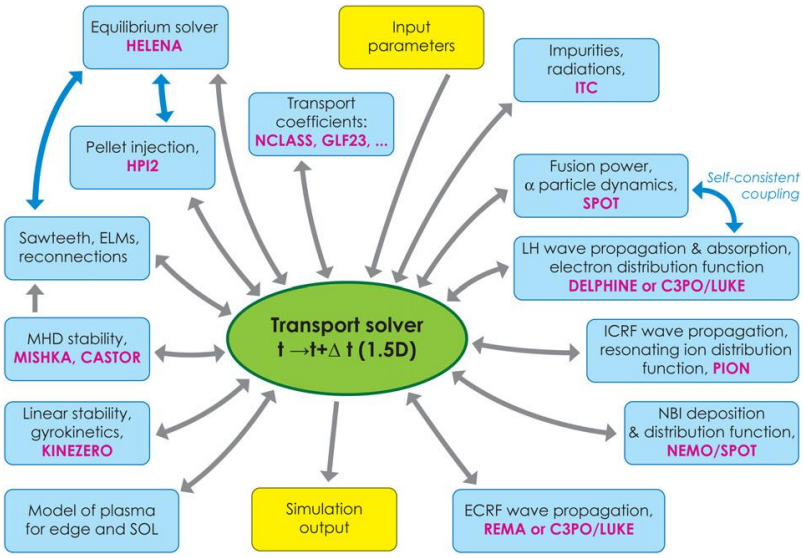

Figure 2.1: The scheme of CRONOS suite of codes; reprinted from [1].

Even though figure (2.1) shows the modular concept of CRONOS, coupling of transport solver core with magnetic equilibrium solver is necessary in order to describe plasma in tokamak. Therefore, the equilibrium solver module should be tightly bonded with transport solver. The basic solver used in CRONOS is fixed-boundary solver HELENA. In order to describe the plasma shape time evolution compatible with circuit equations, free-boundary solver is needed. For plasma shape studies, the CRONOS suite of codes is therefore explicitly coupled with DINA-CH non-linear free-boundary solver through the Simulink. However, there are several problems of this coupling. Firstly DINA-CH is written in Fortran and maintained separately of CRONOS, which is developed in Matlab. Moreover, the data handling between these codes is hard and implicit coupling is de facto impossible. The development of free-boundary solver tightly coupled with CRONOS was therefore needed.

2.2 Free-boundary solver

In numerics, free-boundary problem is more complex than fixed-boundary problem. As their names states, they differ in the knowledge of boundary state and therefore part of the initial state of the described system. As fixed problem has the invariable boundary, its border condition is the only necessity needed in order to solve the problem. On the other hand, the free-boundary problem has to find its boundary as well. Either way, equation describing the problem has to be known.

2.2.1 Magnetic equilibrium

One way of describing plasma is the MHD(Magneto Hydro Dynamics) approach, simplifying the problem by describing it as a conducting fluid. There are several variations of MHD depending on the simplifications made. One of them describes plasma as a single fluid reacting on electromagnetic field. This yields few equations [8], where the one of our interest is force equation, interpreting the third Newton law

$$m\frac{d}{dt}(n\vec{u}) \;=\; mn\frac{\partial \vec{u}}{\partial t} \;+\; mn\,(\vec{u}\cdot\bigtriangledown)\,\vec{u} \;=\; \rho\vec{E} \;+\; \vec{j}\times\vec{B} - \bigtriangledown\cdot\bar{\bar{P}}_0, \tag{2.1}$$

where m stands for mass, n for density, $\vec{u}$ is the flow velocity, t is the time, ρ stands for charge density and $\vec{j}$ current flow, $\vec{E}, \vec{B}$ are electric and magnetic fields and $\bar{\bar{P}}_0$ is the pressure tensor in plasma. In the stationary case without advection, neutrality on macroscopic scale and isotropic plasma pressure, the equation (2.1) results in simple notation

$$\bigtriangledown p \;=\; \vec{j}\times\vec{B}, \tag{2.2}$$

in which $\bigtriangledown p = \bigtriangledown \cdot \bar{\bar{P}}_0$. Dot-product of equation (2.2) with $\vec{B}, \vec{j}$ yields a geometric solution of nested surfaces of constant plasma pressure called magnetic surfaces (visualized in pic.2.2).

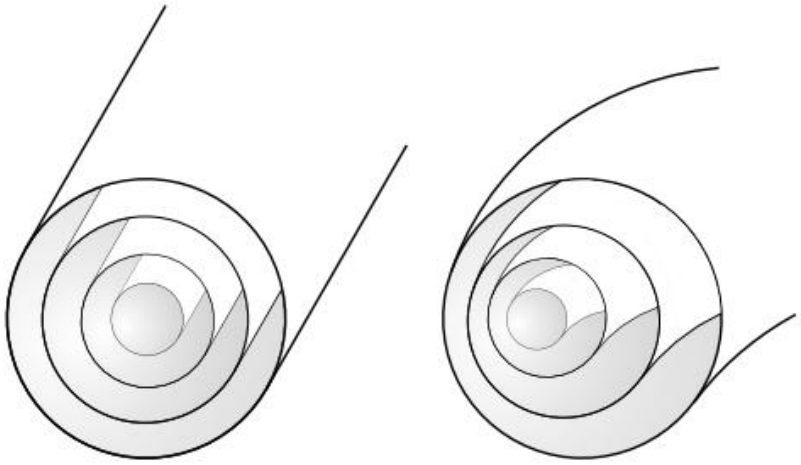

Figure 2.2: Visualization of nested magnetic surfaces in linear and toroidal geometry; reprinted from [11].

Those magnetic surfaces may be characterized by pressure p, toroidal (in the toroid axis direction) Φ and poloidal (around axis, perpendicular to toroidal) Ψ magnetic fluxes. Poloidal magnetic flux Ψ is of greater equation for next derivation and its definition is

$$\Psi = -RA_\varphi, \tag{2.3}$$

in which A_φ is poloidal component of the vector potential.

The description by mentioned magnetic fluxes in cylindrical coordinates yields for the magnetic field

$$\vec{B} = \frac{1}{2\pi R}\left(-\frac{\partial \Psi}{\partial z}, F(\Psi), \frac{\partial \Psi}{\partial R}\right), \tag{2.4}$$

and with the Ampère's circuital law equations for poloidal current density and current density in the z direction

$$
\begin{aligned}
\vec{j} &= \frac{1}{\mu_0}\vec{\bigtriangledown} \times \vec{B}, \\
j_z &= \frac{1}{\mu_0}(\vec{\bigtriangledown} \times \vec{B})_z = \frac{1}{\mu_0 R}\frac{\partial}{\partial R}(RB_\varphi) = \frac{1}{2\pi R\mu_0}\frac{\partial}{\partial R}F(\Psi), \\
j_\varphi &= \frac{1}{\mu_0}(\vec{\bigtriangledown} \times \vec{B})_\varphi = \frac{1}{\mu_0}\left(-\frac{\partial B_r}{\partial z} + \frac{\partial B_z}{\partial R}\right) = \\
&= -\frac{1}{2\pi\mu_0}\left(\frac{1}{R}\frac{\partial^2\Psi}{\partial z^2} + \frac{\partial}{\partial R}\frac{1}{R}\frac{\partial\Psi}{\partial R}\right) = -\frac{1}{2\pi\mu_0 R}\Delta^*\Psi.
\end{aligned} \tag{2.5}
$$

Equation 2.5 is important for next explanation purposes as the theory of Green function is easily applied to it. Considering only the equation with radial derivation of pressure p in equation set (2.2)

$$
\frac{\partial p}{\partial R} = j_\varphi B_z - j_z B_\varphi, \tag{2.6}
$$

and applying previously derived quantities in cylindrical coordinates results in derivation

$$
\begin{aligned}
\frac{\partial p(\Psi)}{\partial R} + \frac{B_z}{2\pi\mu_0 R}\Delta^*\Psi + \frac{B_\varphi}{2\pi R\mu_0}\frac{\partial}{\partial R}F(\Psi) &= 0, \\
\frac{dp(\Psi)}{d\Psi}\frac{\partial\Psi}{\partial R} + \frac{B_z}{2\pi\mu_0 R}\Delta^*\Psi + \frac{B_\varphi}{2\pi R\mu_0}\frac{dF(\Psi)}{d\Psi}\frac{\partial\Psi}{\partial R} &= 0, \times\frac{2\pi\mu_0 R}{B_z}, \\
\Delta^*\Psi + 4\pi^2\mu_0 R^2\frac{dp}{d\Psi} + F(\Psi)\frac{dF(\Psi)}{d\Psi}&,
\end{aligned}
$$

where the last step used the z component of $\vec{B}$ in (2.4) and relation between the poloidal component of magnetic field and current

$$
\begin{aligned}
\frac{\partial\Psi}{\partial R} &= 2\pi R B_z, \\
B_\varphi &= \frac{1}{2\pi R}F(\Psi).
\end{aligned}
$$

by this derivation we obtained the important Grad-Shafranov equation [8]

$$
R\frac{\partial}{\partial R}\left(\frac{1}{R}\frac{\partial\psi}{\partial R}\right) + \frac{\partial^2\psi}{\partial z^2} = -\mu_0 R^2\frac{\partial p}{\partial\Psi} - F(\Psi)\frac{\partial F(\Psi)}{\partial\Psi}, \tag{2.7}
$$

where Ψ is the magnetic poloidal flux, R stands for radial coordinate from toroid axis, z is second basal coordinate of axisymetry plane.

Grad-Shafranov equation is two-dimensional, nonlinear, elliptic partial differential equation for variable Ψ, which is both dependent and independent variable in this equation. The toroidal axis-symmetry is the next assumption for the derivation. This equation is solved as a free-boundary problem by the FREEBIE code.

2.2.2 FREEBIE

As mentioned before, the Grad-Shafranov equation may be solved as fixed boundary problem, i.e. with a given plasma shape, by setting the boundary conditions. These conditions are usually plasma profiles (pressure, poloidal current) or their equivalents. With this input, the Grad-Shafranov equation may be solved for fixed boundary [10].

By allowing the boundary change, an free boundary is obtained and additional information of the system is necessary. This need is primarily satisfied by information of currents in poloidal tokamak systems (active and passive). As the problem is specified, the code implementation is possible.

The FREEBIE code development started at CEA Cadarache and was stand-alone benchmarked for TCV and ITER in 2012. After this, CEA went on with the development of the code by adding additional modes of FREEBIE, the inverse and the unique Poynting modes.

The inverse mode does not use the additional condition of currents in poloidal systems of tokamak, but replaces it with constrains on the plasma shape. As FREEBIE iterates in inverse mode (see fig.2.3) it cannot use circuit equations anymore, but replaces them with an optimizer, which minimizes some quantities of solution, e.g. error in the boundary flux.

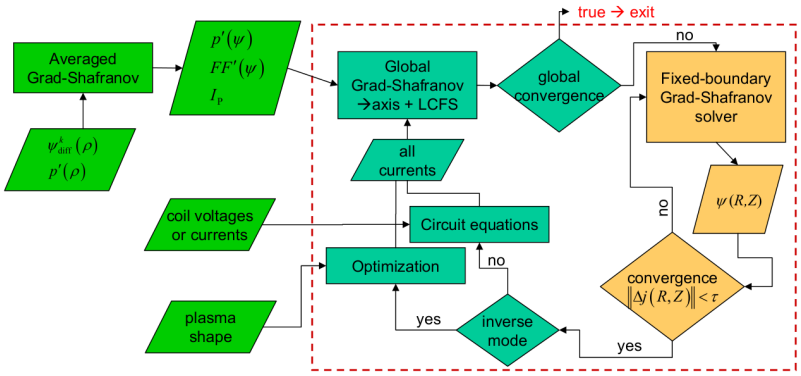

Figure 2.3: Scheme of the FREEBIE code.

As solution of the free-boundary problem extends the fixed-boundary problem in a way, the FREEBIE code is implemented to be able to use de facto any fixed-boundary solver.

This solver has a condition on its boundary in every iteration of FREEBIE. The FREEBIE itself iterates in all modes until the convergence criterion (usually set on averaged plasma current profile) is satisfied.

By satisfaction of the global convergence, the FREEBIE module grants an output of magnetic equilibrium. When coupled with CRONOS suite of codes, FREEBIE is called in every time step. This time step is granted by the solution of transport equations creating CRONOS core. Therefore, the time evolution description of plasma is possible as a sequence of MHD equilibria (the problem is considered as quasi-static) and transport equations solutions [14]. In this meaning, the microscopic MHD equilibrium satisfied in stationary plasma results in macroscopic evolution of plasma shape.

Specifically, the FREEBIE code solves the non-linear Grad-Shafranov PDE by using the Green function. By applying the Green function theory on the Grad-Shafranov equation (2.5), the solution of PDE may be obtained as convolution of Green function with the source term of the equation

$$\psi(R,Z) \;=\; \int_P G(R,Z;R',Z') j_\varphi dR' dZ' + \sum_{i=1}^{N_c} G(R_i^c, Z_i^c; R', Z') I_\varphi, \tag{2.8}$$

where ψ is the poloidal magnetic flux variable used in initial equation (2.5), R, Z are coordinates describing the poloidal cross-section of the tokamak, j_φ stands for the toroidal current density in plasma, N_c is the number of poloidal components (active and passive), G stands for the Green function and I_φ stands for the currents in poloidal components. The integral limit is the plasma boundary, i.e. we integrate over the whole plasma column.

Further on, FREEBIE discretizes the integral into plasma segments. This is done by a triangular grid with high resolution (usage example is on fig.2.4). On such grid, the Green function may be pre-calculated and the solution is therefore much faster.

Yet, as the FREEBIE code is quite young, it is still in development. Goals of this work were to understand the FREEBIE code and contribute to it.

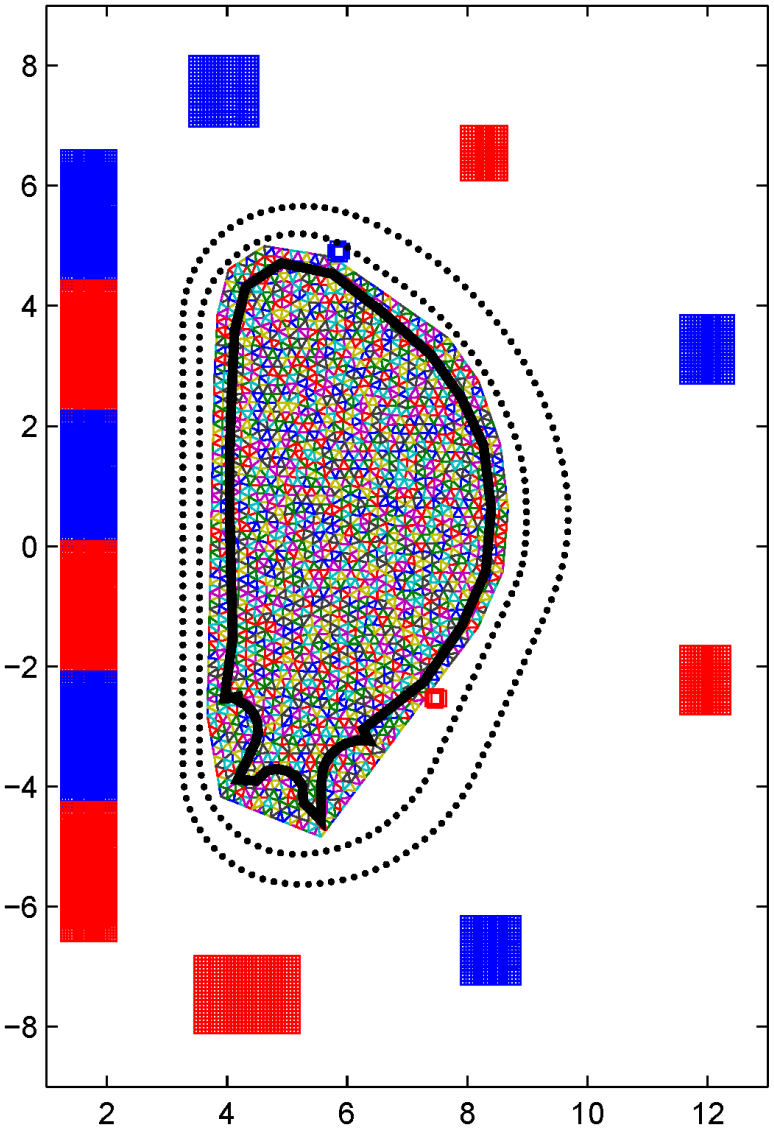

Figure 2.4: An example of triangular grid usage by FREEBIE code; reprinted from [9].

Chapter 3

Author's contribution to the FREEBIE code

As goals of this work states, author's contribution to FREEBIE is divided in two topics. First of them was to implement, test and integrate solver of complex circuits. The second topic focused on fast finding of equipotentials in 2-D function, e.g. spline of an array of poloidal magnetic flux $\Psi(R, Z) = 0$.

3.1 Complex circuits

So far, FREEBIE could describe the poloidal system of coils in tokamak as separated series electrical circuits of an applied voltage and coils. In general the circuits including all poloidal systems(PS) may be more complex, e.g. poloidal systems circuit at tokamak COMPASS visualized in the fig.3.1.

Circuit equations describing the PS used by FREEBIE so far used the matrix description in order to apply specific solvers of such systems, e.g. eigenvalues decomposition and reducing the solution by eigenvalues of less importance. This description

$$\vec{V} + \mathbf{R} \cdot \vec{I} + \mathbf{L}\frac{d\vec{I}}{dt} = \vec{0}, \tag{3.1}$$

where $\vec{V}, \vec{R}$ and $\vec{I}$ stand for the voltage, resistance and current vectors(resistance is a matrix with only diagonal elements, so the final dimension of multiplication yields a vector), describing the circuits as by Kirchhoff circuital law. They are all of dimension n, the number of components to be described. The matrix L is the inductance matrix describing the coils and passive structures self/mutual inductance. This solver has no way how to add the information about the complex circuits, in the simplest example the parallel components.

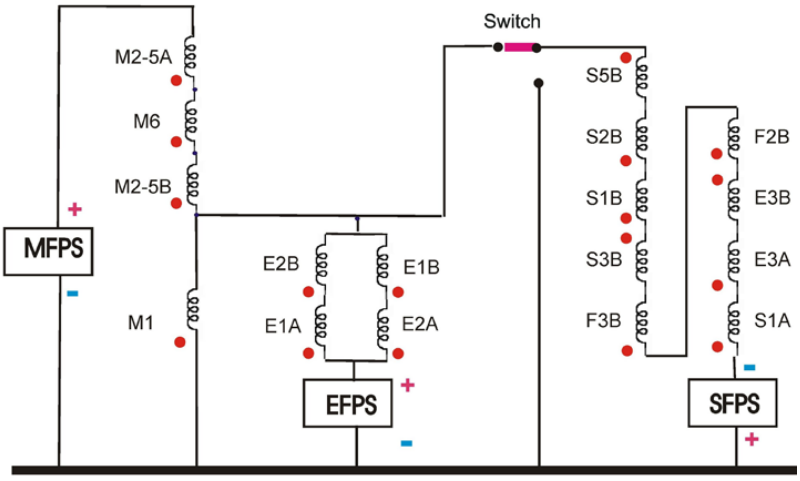

Figure 3.1: Scheme of the real COMPASS circuit for the poloidal systems, reprinted from [6].

In order to describe such circuits, an additional information has to be brought to the system. This information should describe the nodes and their mutual relations. The solution may be found by studying the Kirchhoff voltage law:

> The voltage drop around any loop is zero.

The voltage drop is the difference of potentials, which are the desired solution of problem. Potentials may be used to describe every node and their mutual relations (potential difference due to element between nodes). The system of circuit equations (3.1) may be therefore rewritten in a way of potential description [7]

$$\mathbf{A}\vec{U} = \mathbf{B}\vec{V} + \mathbf{R}\vec{I} + \mathbf{L}\frac{d\vec{I}}{dt}, \tag{3.2}$$

where $\vec{U}$ is newly added vector of potentials at every node and matrices $\mathbf{A}, \mathbf{B}, \mathbf{R}, \mathbf{L}$ are the potential(connection, example of simple set of two circuits in appendix B is shown in 3.3), voltage, resistance and inductance matrices.

$$\mathbf{A} = \begin{pmatrix} \begin{Bmatrix} 1 & -1 & 0 & 0 \\ 0 & 0 & 1 & -1 \\ 1 & -1 & 0 & 0 \\ 0 & 0 & 1 & -1 \end{Bmatrix} \\ \begin{Bmatrix} 0 & 0 & 0 & 0 \\ 0 & 0 & 0 & 0 \\ 0 & 0 & 0 & 0 \\ 0 & 0 & 0 & 0 \end{Bmatrix} \\ \begin{Bmatrix} 0 & 1 & 0 & 0 \\ 0 & 0 & 0 & 1 \end{Bmatrix} \end{pmatrix} \tag{3.3}$$

In matrix $\mathbf{A}$, the first part describes the potentials drop at each component, e.g. for a coil

$$U_i - U_k = RI + L\frac{dI}{dt}. \tag{3.4}$$

The second one is empty due to the whole equation set (3.2) dimension. This equations describe the Kirchhoff's current law in each coil by matrix $\mathbf{R}$. The last equations are definitions of ground potentials for each circuit.

The notable change between (3.1) and (3.2) is that resistance is no longer vector (pure diagonal matrix), but matrix in a normal way. Reason of this fact is easily seen when the dimension analysis of this equation is made. The desired $\vec{I}$ is vector of currents in every component, e.g. coils and passive structures, of dimension n_{comp}. In our new system of equations (3.2), there are n_{nodes} new variables $\vec{U}$. For each of those variables, another equation is needed in order to keep the system regular. Easily obtained equations of same count are Kirchhoff nodal (current) equations. This is the reason for the matrix shape of resistance as this additional laws are described in it. Yet, the problem of potentials is the necessity of setting the zero potential in each described circuit. This yields another $n_{circuit}$ equations. The system is therefore dependent and may be narrowed by $n_{circuit}$ equations, usually taken from the Kirchhoff current law ones.

As the coefficient matrices are by default not square, the derivation of an equation for the current vector is not straightforward. First step is to express vector $\vec{U}$ and plug it back in the system. Even though connection matrix $\mathbf{A}$ is not square, the multiplication with its transpose version is. Such a square matrix may be finally inverted. In this way the potential vector is expressed and by plugging it into the original system of equations (3.2) we can derive matrix description without the potential vector, yet still obtaining the connection matrix information

$$\vec{0} \;=\; \mathbf{E}\vec{V} \;+\; \mathbf{F}\vec{I} \;+\; \mathbf{G}\frac{d\vec{I}}{dt}, \tag{3.5}$$

$$\mathbf{E} \;=\; \mathbf{A}(\mathbf{A}^T\mathbf{A})^{-1}\mathbf{A}^T\mathbf{B} - \mathbf{B}, \tag{3.6}$$
$$\mathbf{F} \;=\; \mathbf{A}(\mathbf{A}^T\mathbf{A})^{-1}\mathbf{A}^T\mathbf{R} - \mathbf{R}, \tag{3.7}$$
$$\mathbf{G} \;=\; \mathbf{A}(\mathbf{A}^T\mathbf{A})^{-1}\mathbf{A}^T\mathbf{L} - \mathbf{L}. \tag{3.8}$$

By following similar steps, the vector $\vec{I}$ in the following form may be derived

$$\vec{I} \;+\; \mathbf{T}\frac{d\vec{I}}{dt} \;=\; \mathbf{S}\vec{V}, \tag{3.9}$$

$$\mathbf{S} \;=\; -(\mathbf{F}^T\mathbf{F})^{-1}\mathbf{F}^T\mathbf{E}, \tag{3.10}$$
$$\mathbf{T} \;=\; (\mathbf{F}^T\mathbf{F})^{-1}\mathbf{F}^T\mathbf{G}. \tag{3.11}$$

3.1.1 Circuit solver results

Previously derived description was implemented and tested on elementary test cases. All models were tested for voltages $V \;=\; 100V$, resistances $R_1 \;=\; 3\Omega$ and $R_2 \;=\; 1\Omega$, self-inductances $L_1 \;=\; L_2 \;=\; \frac{1}{2}H$ and mutual inductance $L_{12} \;=\; -\frac{1}{3}H$. The sign of mutual inductance describes the coil orientation. The case of negative sign corresponds with the case of coils inducing the current corresponding to the orientation of current supplied by the applied voltage. All the test cases were tested against the analytic solution of appropriate circuits, which are derived in appendix B. By each test case, only the result of these derivations are mentioned and the results of testing the numerical model.

At first, the simple current ramp-up of as single coil connected to a voltage was tested (fig.3.2). Its analytic solution

$$I(t) \;=\; \frac{V}{R} - \frac{V}{R}e^{-\frac{R}{L}t}, \tag{3.12}$$

where I, R, L are current, resistance and self-inductance of the coil. V is the voltage source in the circuit.

As the easiest test was successful, testing of parallel circuit as the model's contribution to FREEBIE was the next step. The circuit was extended by parallel coil (fig.3.3) and analytic solution of this circuit is

$$I_2(t) \;=\; \frac{1}{\lambda_2 - \lambda_1}\left(\frac{(L_{12} - L_1)V}{L_{12}^2 - L_1L_2} + \frac{V\lambda_1}{R_2}\right)\left(e^{\lambda_2 t} - e^{\lambda_1 t}\right) - \frac{V}{R_2}e^{\lambda_1 t} + \frac{V}{R_2}, \tag{3.13}$$

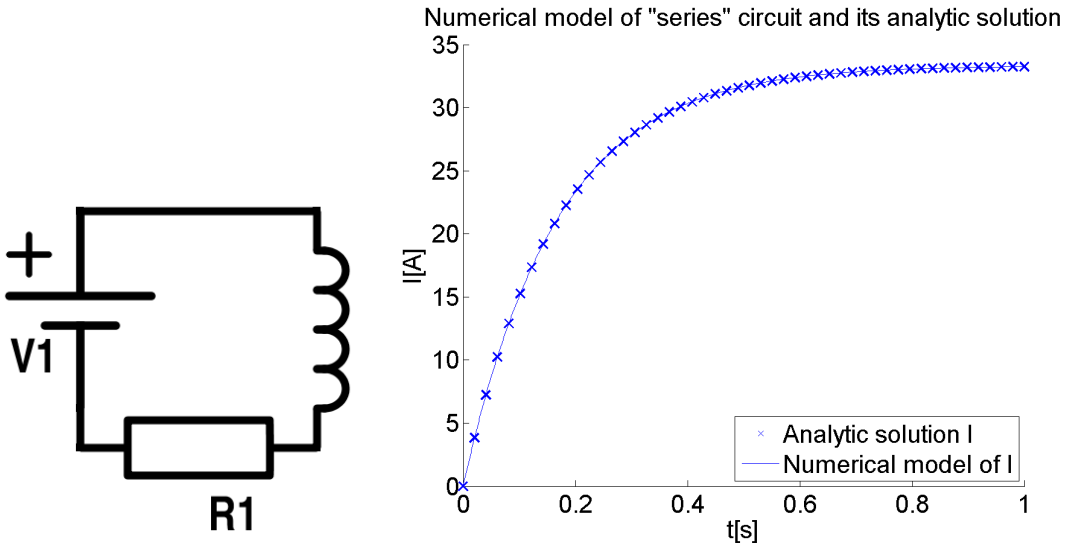

(a) Scheme of simple circuit of coil connected to the voltage; created with [4]. (b) Comparison of the numeric model and the analytic solution $I(t) = \frac{V}{R} - \frac{V}{R}e^{-\frac{R}{L}t}; R = 3\Omega, L = 1/2, V = 100V$.

Figure 3.2: A series circuit scheme and results.

where λ_i are the roots of characteristic equation to the ODE, which is step-by-step derived in appendix mentioned before.

Considering the fact that PS is composed of several poloidal coils, describe them all at once is a desired function. By using the algorithm derived before, any multiple circuits and their bonds may be described. In order to test the numerical model for this function, another test was carried out. Two simple circuits same as in the first example are described connected only by their mutual induction (fig.3.4). Solving this system analytically yields the equation for both coils, e.g. for the second one

$$I_2(t) = \frac{1}{\lambda_2 - \lambda_1}\left(\frac{L_{12}V_1 - L_1V_2}{L_{12}^2 - L_1L_2} + \frac{V_2\lambda_1}{R_2}\right)\left(e^{\lambda_2 t} - e^{\lambda_1 t}\right) - \frac{V_2}{R_2}e^{\lambda_1 t} + \frac{V_2}{R_2}, \tag{3.14}$$

where V_i are the voltages applied in separated circuits.

The last important test to be carried out is the description of passive structures. In these structures, current is induced as if an ideal coil was present and damped by resistance of it (fig.3.5). A practical example is the chamber wall of the tokamak. Analytic solution of current in the passive structure is

$$I_2(t) = \frac{1}{\lambda_1 - \lambda_2}\frac{L_{12}V_1}{L_{12}^2 - L_1L_2}\left(e^{\lambda_1 t} - e^{\lambda_2 t}\right). \tag{3.15}$$

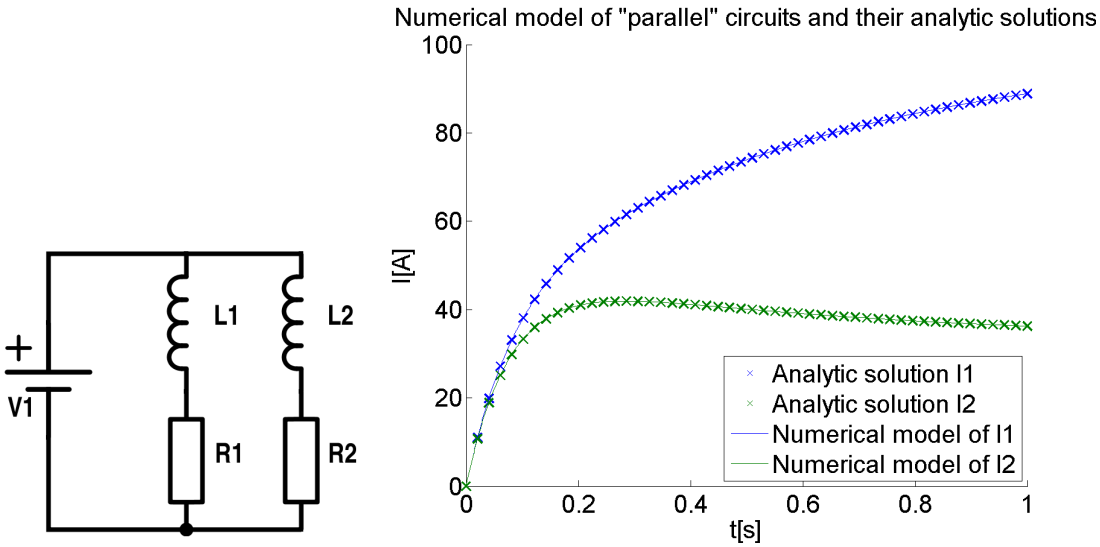

(a) Scheme of simple circuit of two parallel coils connected to the voltage; created with [4].

(b) Comparison of the numeric model and the analytic solution $I_2(t) = \frac{1}{\lambda_2-\lambda_1}\left(\frac{(L_{12}-L_1)V}{L_{12}^2-L_1L_2}+\frac{V\lambda_1}{R_2}\right)\left(e^{\lambda_2 t}-e^{\lambda_1 t}\right)-\frac{V}{R_2}e^{\lambda_1 t}+\frac{V}{R_2}; R_1 = 1\Omega, R_2 = 3\Omega, L_1 = L_2 = \frac{1}{2}H, L_{12} = -\frac{1}{3}H, V = 100V$.

Figure 3.3: A parallel circuit scheme and results.

3.2 Equipotential finder

The second task of the contribution was to create a stand-alone tool for finding equipotentials of a function. The main motivation of this task was the need of finding magnetic surfaces in poloidal cross-section of tokamak, i.e. equipotentials in 2-D function of Ψ. This tool is meant to be used by FREEBIE to process the equilibrium data. Although there are programming languages, which include a function for easy and fast equipotential plotting, acquiring the data from the results is slow in order to be used in the FREEBIE computational core. Moreover, as FREEBIE discretizes the plasma column to a triangular grid (fig.2.4), the data output is in a form of an array, which needs to be interpolated first. The convenience of creating a new solver is also the consistency of FREEBIE by using the same spline for every module used.

In order to find a equipotential of a given function, the implicit function theory is first to look at solution. Problem with the implicit solution is the turnarounds in specific coordinates, where the division by zero throws an error. This problem has an elegant workaround of additional dependency of coordinates [12]. The addition of one more variable in the system needs to be compensated by adding one more equation, giving the new variable a physical meaning. In our case, the dependency is on the variable λ, which is given the meaning of the equipotential length.

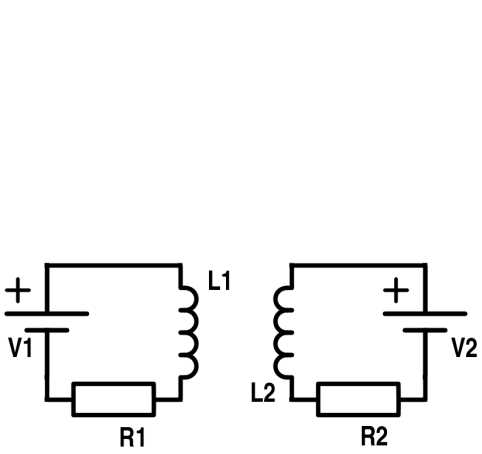

(a) Scheme of two simple circuits connected only by mutual induction of coils; created with [4].

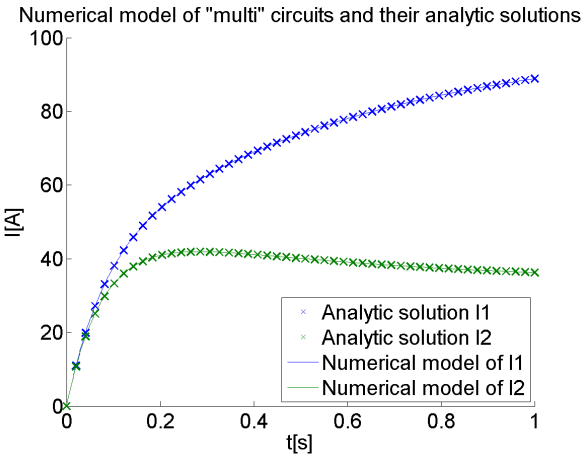

(b) Comparison of the numeric model and the analytic solution $I_2(t) = \frac{1}{\lambda_2-\lambda_1}\left(\frac{L_{12}V_1-L_1V_2}{L_{12}^2-L_1L_2} + \frac{V_2\lambda_1}{R_2}\right)\left(e^{\lambda_2 t} - e^{\lambda_1 t}\right) - \frac{V_2}{R_2}e^{\lambda_1 t} + \frac{V_2}{R_2}; R_1 = 1\Omega, R_2 = 3\Omega, L_1 = L_2 = \frac{1}{2}H, L_{12} = -\frac{1}{3}H, V_1 = V_2 = 100V.$

Figure 3.4: Two series circuits with a bond scheme and result of the numerical solver.

$$F(x,y) = 0, \tag{3.16}$$

$$\frac{\partial F}{\partial x}\frac{dx}{d\lambda} + \frac{\partial F}{\partial y}\frac{dy}{d\lambda} = 0, \tag{3.17}$$

$$(d\lambda)^2 = (dx)^2 + (dy)^2, \tag{3.18}$$

where $F(x,y)$ is in general the described 2-D function with dependency on its coordinates x, y, which has further dependency on the curve length α. By separating the proper derivations, a set of equations for each coordinate is obtained.

$$\frac{dx}{d\lambda} = \mp\frac{F_y}{\sqrt{F_x^2+F_y^2}},\ x(0) = x_0, \tag{3.19}$$

$$\frac{dy}{d\lambda} = \pm\frac{F_x}{\sqrt{F_x^2+F_y^2}},\ y(0) = y_0. \tag{3.20}$$

$$\tag{3.21}$$

By evaluating these equations, which cannot in normal cases encounter the division by zero, the problem is solved. In special case of tokamak application, the function F is equivalent to the function Ψ and coordinates are R, Z. This special case was used

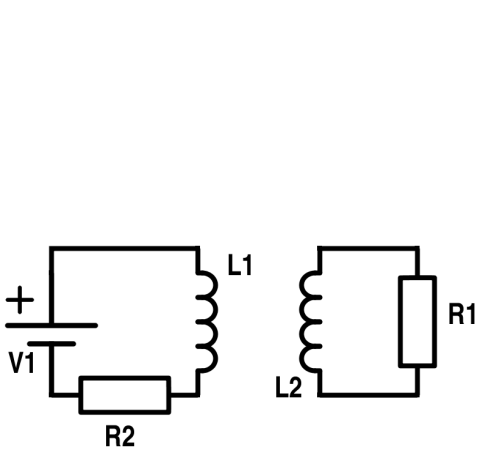

(a) Scheme of passive structure influenced by an simple circuit with a coil; created with [4].

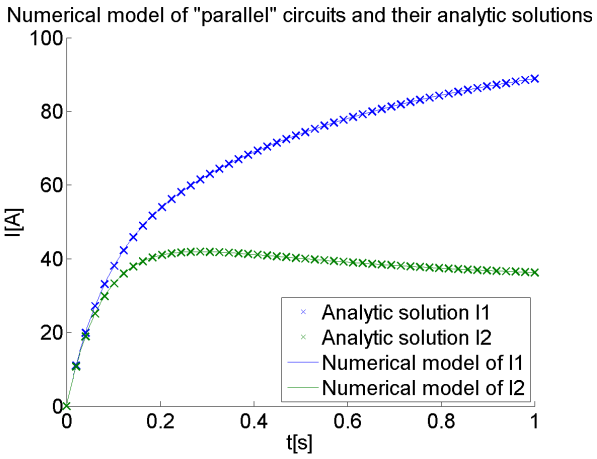

(b) Comparison of the numeric model and the analytic solution $I_2(t) = \frac{1}{\lambda_1-\lambda_2}\frac{L_{12}V_1}{L_{12}^2-L_1L_2}\left(e^{\lambda_1 t}-e^{\lambda_2 t}\right); R_1 = 1\Omega, R_2 = 3\Omega, L_1 = L_2 = \frac{1}{2}H, L_{12} = -\frac{1}{3}H, V_1 = 100V$.

Figure 3.5: A series circuit bonded to a passive structure scheme and results of the numerical solver.

to benchmark the algorithm to the contour plot function of matplotlib.pyplot package (fig.3.6). The algorithm itself is written as an python stand-alone package imported by FREEBIE.

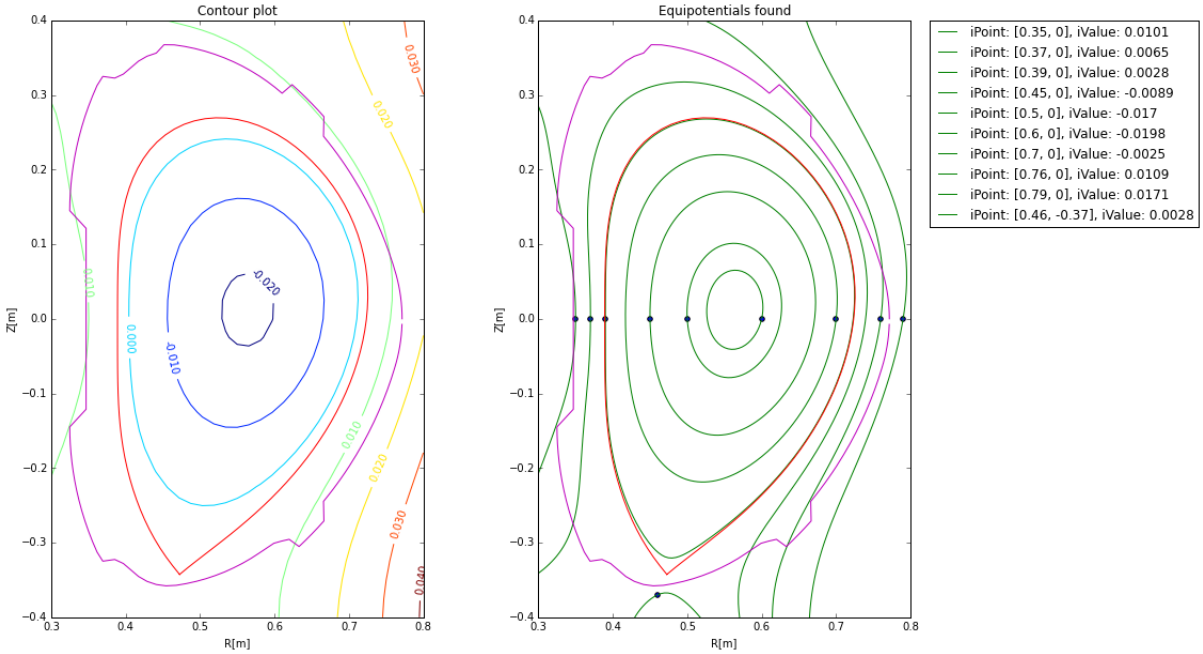

Figure 3.6: Comparison of contour plot(left) and algorithm results(right); The function shown is $\Psi(R, Z)$ in tokamak COMPASS, the purple line visualizes the tokamak chamber and the red one is the last closed flux surface (LCFS).

Summary

Summary

The CRONOS suite of codes for tokamak discharge simulation needs an free-boundary equilibrium solver. Therefore, the recently benchmarked FREEBIE code is developed. This work consists of implementation of the code for complex electrical circuit description of poloidal systems, as FREEBIE method used so far could describe only series circuits. This newly implemented description uses the potential description of the circuit. Few tests of basic circuits were run and the results of implemented numerical solver were compared to analytic solutions of these circuits with success.

Next contribution of this work is creation of python module of equipotential finder. This module is the base of future package for external equilibria data processing. Equipotential finder was benchmarked for the python matplotlib.pyplot module's function contour plot. The benefit of newly implemented equipotential finder is its speed of computation data retrieving and usage of general spline class. Therefore, future package may use spline class for FREEBIE output array consistent with FREEBIE.

Bibliography

[1] J.F. Artaud et al. "The CRONOS suite of codes for integrated tokamak modelling". In: *Nuclear Fusion* 50.4 (2010), s. 043001.

[2] *Confinement and Trasnsport*. 2015. URL: https://fusion.gat.com/iter/iter-ga/confinement_transport.html (cit. 22. 09. 2015).

[3] New World Encyclopedia contributors. *Nuclear Fusion*. 2015. URL: http://www.newworldencyclopedia.org/entry/Nuclear_fusion (cit. 22. 09. 2015).

[4] DigiKey. *Scheme-it, Design and Share Schematics*. URL: http://www.digikey.com/schemeit/ (cit. 22. 09. 2015).

[5] GOLEM@FJFI.CVUT. *Physical principle of tokamaks*. 2008. URL: http://golem.fjfi.cvut.cz/?p=documentation_tokamak_overall (cit. 22. 09. 2015).

[6] J. HAVLICEK, R. BEŇO a J. STÖCKEL. "A Simulation of the COMPASS Equilibrium Field Power Supply PID Controller". In: *Matfyzpress* (2011). ISBN 978-80-7378-185-9, s. 221–226.

[7] Holger Heumann et al. "Quasi-static Free-Boundary Equilibrium of Toroidal Plasma with CEDRES++: Computational Methods and Applications". In: *Journal of Plasma Physics* (2015). DOI: 10.1017/S0022377814001251.

[8] S. Jardin. *Computational methods in plasma physics*. ISBN 978-143-9810-958. 2010.

[9] J.Urban a J.-F.Artaud. *Coupled Transport and Free-boundary Equilibrium Simulations using FREEBIE and CRONOS*. 2012.

[10] J.Urban et al. *Status and Benchmarking of the Free Boundary Equilibrium Code FREEBIE*. Poster presented at BAPS conference. 2013.

[11] Jindřich Kocman. "Zpětnovazební řízení polohy na tokamaku GOLEM". Dipl. Czech Technical University in Prague, 2011. URL: http://physics.fjfi.cvut.cz/publications/FTTF/BP_Jindrich_Kocman.pdf.

[12] E.B. Kuznetsov. "Optimal parametrization in numerical construction of curve". In: *Journal of the Franklin Institute* 344.5 (2007), s. 658–671.

[13] *Plasma physics: at the heart of fusion.* 2015. URL: http://ec.europa.eu/research/energy/euratom/index_en.cfm?pg=fusion&section=plasma-physics (cit. 22. 09. 2015).

[14] S.C.JARDIN. "Some Considerations and Techniques for the Predictive Simulation of Global Instabilities in Tokamaks". In: *Fusion Science and Technology* 59.3 (2010), s. 519–525.

Appendix

Appendix A

Table of variables

Variable	Basic unit	Name
E	[J]	Energy
Δm	[kg]	Mass diference
τ_E	[s]	Confinement time
W_P	[J]	Plasma energy
P_L	[W]	Plasma power losses
n_i	[m^{-3}]	Density of i component in fusion reaction
n_D	[m^{-3}]	Density of deuterium fuel
n_T	[m^{-3}]	Density of tritium fuel
T	[eV]	Temperature
σ	[barn]	Nuclear cross-section
v_r	[ms^{-1}]	Relative velocity
ε_f	[-]	Energy gain from one reaction
P_i	[W]	Internal heat power
R	[m]	Radius from the tokamak axis, major radius
B_t	[T]	Toroidal component of the magnetic field
P_H	[W]	Heat power
m	[kg]	mass
$\vec{u}$	[ms^{-1}]	flow velocity
t	[s]	Time
E	[Vm^{-1}]	Electric field
B	[T]	Magnetic field
j	[Am^{-2}]	Current density
ρ	[kgm^{-3}]	Mass density
$\bar{\bar{P}}_0$	[Pa]	Pressure tensor

Variable	Basic unit	Name
Ψ_θ	[]	Toroidal magnetic flux
Ψ_ϕ	[]	Poloidal magnetic flux
I_p	[A]	Plasma current
G	[-]	Green's function
N_c	[-]	Number of coils
$\vec{V}$	[V]	Voltage vector
$\vec{I}$	[A]	Current vector
$\mathbf{L}$	[H]	Inductance matrix
$\mathbf{R}$	[Ω]	Resistance matrix
$\vec{U}$	[V]	Potential vector
$\mathbf{A}$	[-]	Circuit connection matrix
$\mathbf{B}$	[-]	Voltage matrix
n_{nodes}	[-]	Number of nodes in described set of circuits
n_{comp}	[-]	Number of components in described set of circuits
n_{circ}	[-]	Number of circuits in described set of circuits
λ_i	[-]	Eigenvalues of the characteristic equation for described ODE
F	[-]	General 2-D function
F_x	[-]	Derivation of F by variable x
F_y	[-]	Derivation of F by variable y

Table of constants

Variable	Approximate value	Name
π	3.1415926	Pi
c	299792458 ms^{-1}	Speed of light
μ_0	1.2566370×10^{-6} $\mathrm{VsA}^{-1}\mathrm{m}^{-1}$	Vacuum permeability

Appendix B

Analytic solutions

B.1 A series circuit

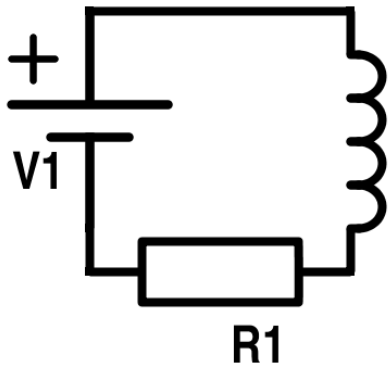

Figure B.1: Scheme of simple series circuit; created via [5].

By applying the Kirchhoff's circuital law an ordinary differential equation (ODE) with constant coefficients for the current in the coil I is obtained.

$$V = RI + L\frac{dI}{dt} \tag{B.1}$$

This ODE's characteristic equation leads to a fundamental system FS

$$L\lambda + R = 0 \tag{B.2}$$

$$\lambda = -\frac{R}{L} \tag{B.3}$$

$$FS = \left\{e^{\lambda t}\right\}. \tag{B.4}$$

The particular solution PS is the simplest solution of equation (B.1)

$$I_{PS} = \frac{V}{R}. \tag{B.5}$$

By combining the FS with the PS and the initial solution of the relaxed circuit without supply ($I(0) = 0A$) the final solution is obtained.

$$I(t) = \frac{V}{R} - \frac{V}{R}e^{-\frac{R}{L}t} \tag{B.6}$$

B.2 Two separated circuits with a bond

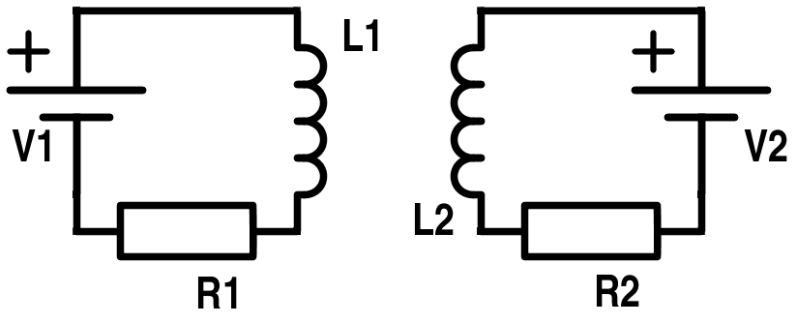

Figure B.2: Scheme of two simple circuits bounded by coils mutual inductance; created via [5].

By applying the Kirchhoff's circuital law a set of ordinary differential equations (ODEs) for currents in coils I_1, I_2 is obtained.

$$V_1 = R_1 I_1 + L_1\frac{dI_1}{dt} + L_{12}\frac{dI_2}{dt} \tag{B.7}$$

$$V_2 = R_2 I_2 + L_2\frac{dI_2}{dt} + L_{12}\frac{dI_1}{dt} \tag{B.8}$$

This two equations are mutually bounded and for the solution separated equations for the currents are needed. One way of obtaining such separated equations is the multiplication of the first equation by coefficient L_{12}, second by the coefficient L_1 and by subtracting the second equation from the first. These steps yields an equation where the variable I_1 may be separated as follows

$$I_1 = \frac{L_{12}V_1 + L_1R_2I_2 + (L_1L_2 - L_{12}^2)\frac{dI_2}{dt}}{L_{12}R_1}. \tag{B.9}$$

Such separated current yields a second order differential equation about I_2 when combined with the first of equations (B.7).

$$V_2 = R_2I_2 + \left(L_2 + \frac{L_1R_2}{R_1}\right)\frac{dI_2}{dt} + \left(\frac{L_1L_2 - L_{12}^2}{R_1}\right)\frac{d^2I_2}{dt^2} \tag{B.10}$$

Equation (B.10) is a ODE with constant coefficients and can be therefore solved by finding roots of its characteristic equation

$$K_1\lambda^2 + K_2\lambda + R_2 = 0, \tag{B.11}$$

$$\lambda_{1,2} = \frac{-K_2 \pm \sqrt{K_2^2 - 4K_1R_2}}{2K_1}, \tag{B.12}$$

where K_1 and K_2 are coefficients by the derivations in equation (B.10). Fundamental system of equation (B.10) is therefore

$$FS = \left\{e^{\lambda_1 t}, e^{\lambda_2 t}\right\}. \tag{B.13}$$

The particular solution is easily obtained by finding the linear solution

$$I_{PS} = \frac{V_2}{R_2}. \tag{B.14}$$

And the solution of the ODE therefore is

$$I(t) = C_1e^{\lambda_1 t} + C_2e^{\lambda_2 t} + \frac{V_2}{R_2}. \tag{B.15}$$

The constants C_1 and C_2 may be specified by the initial conditions of the system. Basic one is that the circuit is not charged at the time $t = 0s$. The second condition may be calculated from equation (B.9). By observing the situation at $t = 0$, where both I_1 and I_2 are equal to zero, we could determine the initial condition for the derivation of I_2. Using these conditions specifies the constants and results in the solution

$$I_2(t) = \frac{1}{\lambda_2 - \lambda_1}\left(\frac{L_{12}V_1 - L_1V_2}{L_{12}^2 - L_1L_2} + \frac{V_2\lambda_1}{R_2}\right)\left(e^{\lambda_2 t} - e^{\lambda_1 t}\right) - \frac{V_2}{R_2}e^{\lambda_1 t} + \frac{V_2}{R_2}. \tag{B.16}$$

B.3 Circuit with parallel components

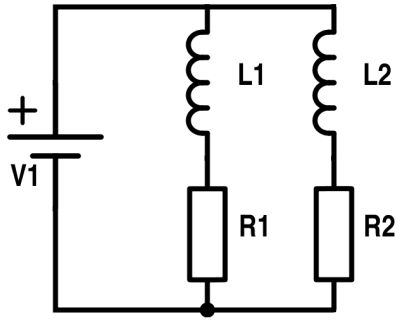

Figure B.3: Scheme of simple circuit with parallel coils; created via [5].

By applying the Kirchhoff's circuital law a set of ordinary differential equations (ODEs) for currents in coils I_1, I_2 is obtained.

$$V = R_1 I_1 + L_1 \frac{dI_1}{dt} + L_{12} \frac{dI_2}{dt} \tag{B.17}$$

$$V = R_2 I_2 + L_2 \frac{dI_2}{dt} + L_{12} \frac{dI_1}{dt} \tag{B.18}$$

This set of equations is the same as for the separated circuits in the case of same voltages $V_1 = V_2 \equiv V$. The solution is therefore the same with specified voltages and results in

$$I_2(t) = \frac{1}{\lambda_2 - \lambda_1} \left(\frac{(L_{12} - L_1)V}{L_{12}^2 - L_1 L_2} + \frac{V \lambda_1}{R_2} \right) \left(e^{\lambda_2 t} - e^{\lambda_1 t} \right) - \frac{V}{R_2} e^{\lambda_1 t} + \frac{V}{R_2}. \tag{B.19}$$

B.4 Circuit with a passive structure

By applying the Kirchhoff's circuital law a set of ordinary differential equations (ODEs) for currents in coils I_1, I_2 is obtained.

$$V_1 = R_1 I_1 + L_1 \frac{dI_1}{dt} + L_{12} \frac{dI_2}{dt} \tag{B.20}$$

$$0 = R_2 I_2 + L_2 \frac{dI_2}{dt} + L_{12} \frac{dI_1}{dt} \tag{B.21}$$

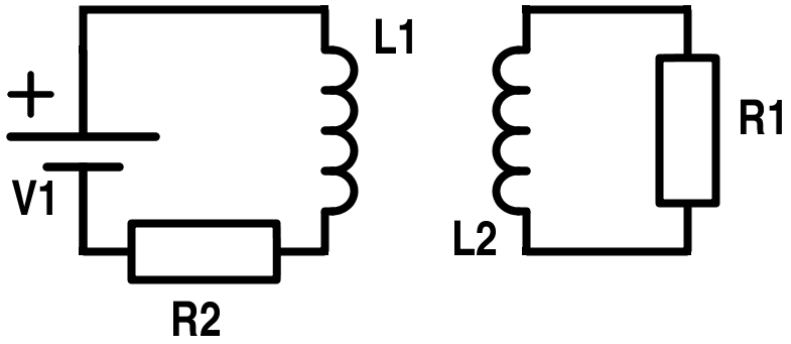

Figure B.4: Scheme of a simple circuit and a passive structure; created via [5].

This two equations are mutually bounded and for the solution separated equations for the currents are needed. One way of obtaining such separated equations is the multiplication of the first equation by coefficient L_{12}, second by the coefficient L_1 and by subtracting the second equation from the first. These steps yields an equation where the variable I_1 may be separated as follows

$$I_1 \;=\; \frac{L_{12}V_1 \;+\; L_1R_2I_2 \;+\; (L_1L_2 \;-\; L_{12}^2)\frac{dI_2}{dt}}{L_{12}R_1}. \tag{B.22}$$

Such separated current yields a second order differential equation about I_2 when combined with the second of equations (B.21).

$$0 \;=\; R_2I_2 \;+\; \left(L_2 \;+\; \frac{L_1R_2}{R_1}\right)\frac{dI_2}{dt} \;+\; \left(\frac{L_1L_2 - L_{12}^2}{R_1}\right)\frac{d^2I_2}{dt^2} \tag{B.23}$$

Equation (B.23) is a homogeneous ODE with constant coefficients and can be therefore solved by finding roots of its characteristic equation

$$K_1\lambda^2 \;+\; K_2\lambda \;+\; R_2 \;=\; 0, \tag{B.24}$$

$$\lambda_{1,2} \;=\; \frac{-K_2 \pm \sqrt{K_2^2 - 4K_1R_2}}{2K_1}, \tag{B.25}$$

where K_1 and K_2 are coefficients by the derivations in equation (B.23). Fundamental system of equation (B.23) is therefore

$$FS \;=\; \left\{e^{\lambda_1 t}, e^{\lambda_2 t}\right\}. \tag{B.26}$$

As the equation is homogeneous, its particular solution is trivial and the solution is

$$I(t) \;=\; C_1 e^{\lambda_1 t} \;+\; C_2 e^{\lambda_2 t}. \tag{B.27}$$

The constants C_1 and C_2 may be specified by the initial conditions of the system. Basic one is that the circuit is not charged before time $t \;=\; 0\ s$. The second condition may be calculated from equation (B.22). By observing the situation at $t \;=\; 0$, where both I_1 and I_2 are equal to zero, we could determine the initial condition for the derivation of I_2. Using these conditions specifies the constants and results in solution

$$I_2(t) \;=\; \frac{1}{\lambda_1 - \lambda_2} \frac{L_{12} V_1}{L_{12}^2 - L_1 L_2} \left(e^{\lambda_1 t} - e^{\lambda_2 t} \right). \tag{B.28}$$